Effect of *van der Waals* interaction on the properties of SnS_2 layered semiconductor

Y. Seminovski P. Palacios P. Wahnón

A B S T R A C T

Nowadays, dispersion correction applied on layered semiconductors is a topic of interest. Among the known layered semiconductors, SnS_2 polytypes are wide gap semiconductors with a *van der Waals* interaction between their layers, which could form good materials to be used in photovoltaic applications. The present work gives an approach to the SnS_2 geometrical and electronic characterization using an empirical dispersion correction added to the Perdew–Burke–Ernzerhof functional and subsequent actualization of the electronic charge density using the screened hybrid Heyd–Scuseria–Ernzerhof functional using a density functional code. The obtained interlayer distance and band-gap are in good agreement with experimental values when *van der Waals* dispersion forces are included.

1. Introduction

The SnS_2 presents a CdI_2 layered type structure, and also has polytypism [1,2] in which the perpendicular stacking of the layers is different in each polytype. Intra-layer bonds are rather strong due to the covalent nature within, thus the *van der Waals* (vdW) interaction among the layers is weaker than that of the intra-layer bonds. This phenomenon permits a deformation of the structure by using a slightly strong force [3–6], which can be translated as a phase equilibrium named polytypism. It is reported that the 2H polytype is the most stable when the synthesis occurs at low temperature, 18R at medium temperature and 4H when the synthesis temperature is above 800 °C [7,8].

Low cost and easy synthesis routes in SnS_2 [9] make the possibility of using this material in different applications among which is the use of SnS_2 as a photovoltaic material [10–12] and in this area recently SnS_2-4H doped with V had been proposed as an intermediate band material for solar cells [13].

In this work the 2H and 4H SnS_2 polytypes are theoretically studied and compared using Density Functional Theory (DFT) with and without the inclusion of a vdW dispersion correction in the calculations. The need of this term will be demonstrated with geometric and electronic structure results.

2. Structure and computational details

DFT Vienna Ab initio simulation package (VASP) calculations, with projector augmented wave (PAW) potentials [14,15] and Perdew–Burke–Ernzerhof (PBE) Generalized Gradient Aproximation (GGA) functional [16] using a $8\times8\times6$ Monkhorst–Pack grid of k points, including volume relaxation were made for the SnS_2 polytypes. Band and projected band calculations were made using the high symmetry k point that corresponds to each polytype. The cut-off energy used, 360 eV, was high enough to evaluate the convergence of each of the studied materials. The small energy difference to consider convergence was $\pm1\cdot10^{-3}$eV, and the energy difference to achieve the lowest energy in the system was $\pm1\cdot10^{-7}$eV. Further calculations using the screened hybrid Heyd–Scuseria–Ernzerhof (HSE) functional without additional relaxation [17,18] were held to obtain SnS_2 2H and 4H accurate band-gaps.

Grimme empirical dispersion correction [19] was made using identical $s_6=0.75$ parametrization in both the methods PBE and HSE. The used cells in each case correspond with the unit cell of each structure, taking into account the experimental parameters. These 2H and 4H polytypes respectively crystallize in hexagonal P-3m1 and $P6_3mc$ space group and the structures are depicted in Fig. 1a and b.

3. Results and discussion

After geometric and electronic convergence of all supercell structures, the resulting geometric *a* and *c* lattice parameters within the two SnS_2 polytypes studied, 2H and 4H and using DFT method with and without vdW dispersion correction, can be seen in Table 1. The results obtained were corroborated using different sized supercells up to hundred of atoms. We can observe in Fig. 1 that the stacking of the layers appears along the *c* parameter of the cells. Furthermore, 2H and 4H polytypes are identical except for the displacement of the second layer in the latter. The interlayer distance is the same in the two cases, and the experimental value reported is 0.586 nm. We

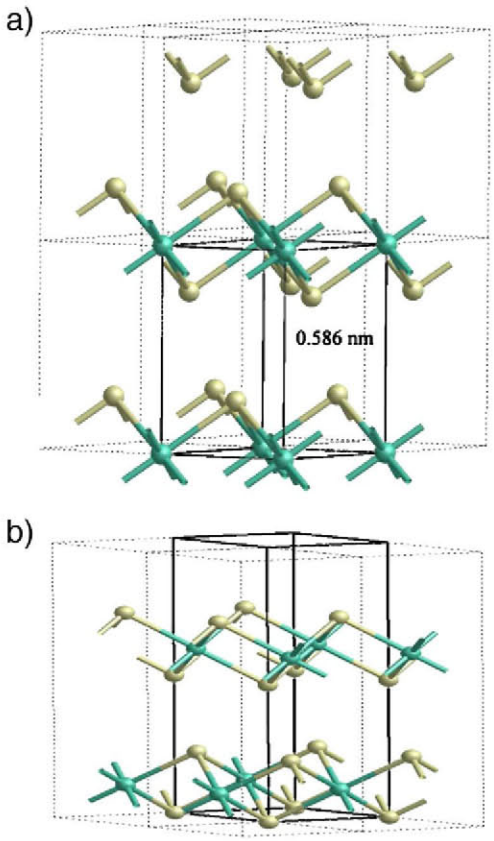

Fig. 1. 2×2×2 expansion of the primitive unit cell of 2H (a) and 4H (b) symmetry in SnS_2 polytypes. Interlayer distance (d) can be observed in the 2H case.

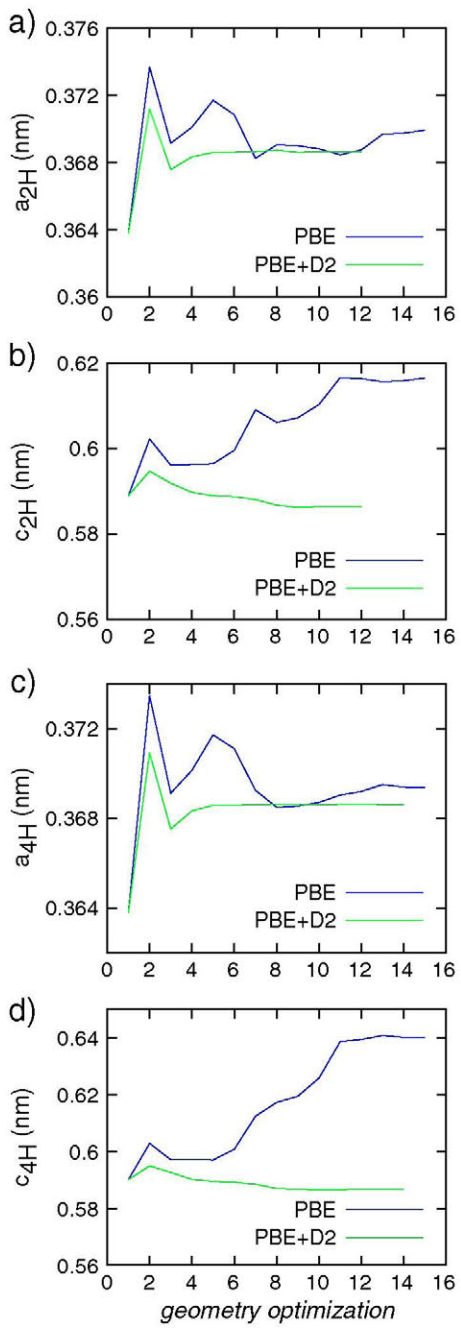

Fig. 2. Evolution of lattice parameters a, c for 2H (subfigures a and b) and 4H (subfigures c and d) polytypes respectively through relaxation calculations.

can observe that the best fit of the geometry corresponds with the cases that include vdW dispersion correction, comparing with experimental values [3]. The calculations without taking into account the vdW interactions have an increased c lattice parameter as a result of the dismissed weak vdW interaction between the layers (Fig. 2b and d), due to the fact that no chemical bonds are attached to the layers. Furthermore, the lattice parameter perpendicular to the stacking direction is quite well reproduced in GGA calculations (Fig. 2a and c).

These demonstrate that GGA (without using dispersion corrections) gives a volume expansion for the c lattice parameter and the resulting interaction between the layers is a repulsion. This tendency is corrected using Grimme empirical method after each auto-consistent cycle. For the a parameter direction we do not have predominant dispersion forces, so both approaches give a similar result. The good agreement found between experimental and computed c parameters when Grimme's correction is introduced means that the possible inadequacy [20] of applying to a strongly polar or ionic compound (as is the case here) the original Grimme's parameters, which are appropriate for neutral atoms, is not a problem in the present case [21].

Table 1
Lattice parameters of SnS_2 2H and 4H using different methods.

	a (nm)	c (nm)
EXP [3]	0.364	1.180
2H (PBE)	0.370	1.333
2H (PBE + D2)	0.369	1.178
4H (PBE)	0.370	1.338
4H (PBE + D2)	0.369	1.178

We also have obtained the band diagrams (Fig. 3) of the two polytypes using GGA–PBE (Fig. 3a and c) and GGA with dispersion correction (PBE + D2) (Fig. 3b and d). The effect of the Grimme dispersion correction in the band dispersion is only related with a decreased energy of each band relative to the upper edge of the valence band, but the shape of the dispersion remains similar. Furthermore after the geometry optimization with PBE and PBE + D2, the HSE update of the density matrix was obtained and included also the dispersion correction HSE + D2.

As can be expected HSE corrects the PBE band-gap. The effect of vdW correction in HSE calculations is similar to what happens in PBE calculations. We found a decrease in band energies and the shape of the bands remains the same. These results can be seen in Fig. 3. An interesting observation relates to the dispersion curves in

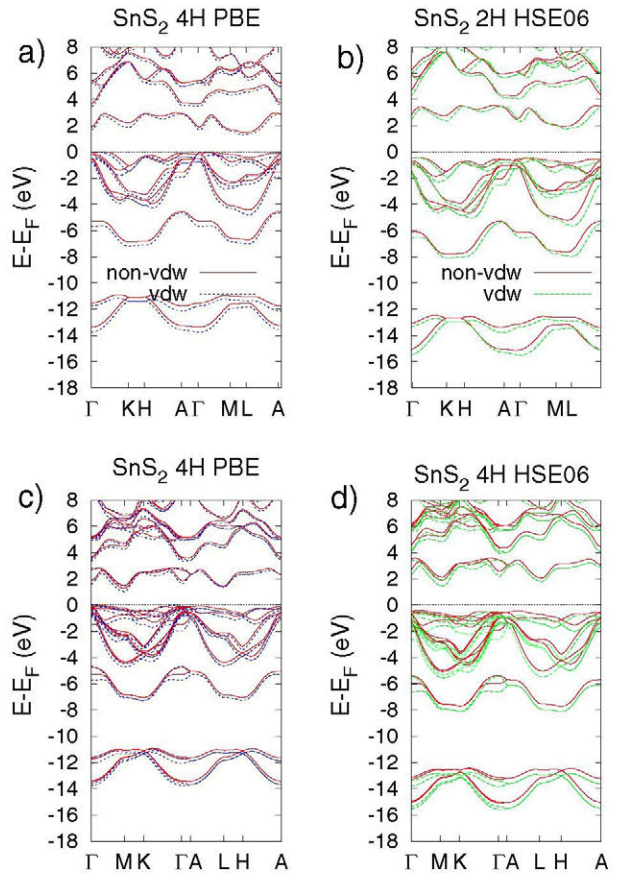

Fig. 3. Energy band diagrams of SnS_2 2H (subfigures a and b) and 4H (subfigures c and d) polytypes, with (dashed lines) and without dispersion correction (solid lines). Comparison of PBE (subfigures a and c) and HSE (subfigures b and d) method results.

the segment between the Γ point and point A, which is the direction perpendicular to the layers; in this segment the bands are not flat (as would be expected for a purely 2D system without electronic overlap between layers) even in the GGA-optimized geometry which yields a large interlayer separation, implying that also in this latter case there is significant electronic interaction between layers. As could be expected, the band dispersion in this segment increases significantly when the layers approach due to the inclusion of the *van der Waals* effect. All these results can be seen in Fig. 3.

In Table 2 we show the obtained direct and indirect band-gaps ($E_{g,dir}$ and $E_{g,ind}$) for the 2H and 4H SnS_2 polytypes with the PBE and HSE functionals and with and without applying the Grimme method. Theoretical band-gaps are compared with experimental results. As is expected PBE results underestimate the band-gaps in both systems and this problem is not solved with a dispersion correction which allows us to obtain good geometrical results. HSE calculations correct band-gaps but the obtained results are overestimated in comparison to the experiment due to the lack of dispersion correction which corrects the stacking distance. If we combine both HSE and vdW dispersion corrections (HSE + D2), theoretical band-gaps agree quite well with experimental data.

Table 2
Direct and indirect energy gaps (experimental value in parentheses) in SnS_2 2H and 4H polytypes. $E_{g,ind}$ is respectively calculated from Γ-L and Γ-M transition for 2H and 4H.

SnS_2	Method	$E_{g,ind}$ PBE (eV)	$E_{g,ind}$ HSE (eV)	$E_{g,dir}$ HSE (eV)
2H	DFT	1.50	2.37 (2.18 [22])	3.17 (2.56 [23])
	DFT + $D2_{Grimme}$	1.32	2.20 (2.18)	2.80 (2.56)
4H	DFT	1.30	2.28 (1.89 [22])	3.04 (2.43 [23])
	DFT + $D2_{Grimme}$	1.05	1.97 (1.89)	2.73 (2.43)

4. Conclusions

The dispersion corrections were applied for the 2H and 4H SnS_2 layered polytypes. The resulting lattice parameters and the indirect and direct band-gaps were obtained using PBE and HSE functionals. Interlaying spacing results are in good agreement with experimental values when dispersion force corrections are applied, including both this effect and the HSE functional gives the best agreement of the computed band gap with experiment. Band dispersions along the main directions for the different functionals are compared with results adding a vdW correction. The shape and width of the bands remain nearly unchanged and we found a decrease in energy for the corrected bands relative to the valence band upper edge.

Acknowledgments

We wish to thank Professor J.C. Conesa for his critical reading of the manuscript and active discussion during this work. Also we would like to acknowledge the funding from the FOTOMAT project (Grant No. MAT2009-14625-C03-01) and the Comunidad de Madrid NUMANCIA2 project (S-2009ENE-1477). Authors thankfully acknowledge the computer resources, technical expertise and assistance provided by the Centro de Supercomputación y Visualización de Madrid (CeSViMa) and the Spanish Supercomputing Network.

References

[1] R.S. Mitchell, Y. Fujiki, Y. Ishizawa, Nature 247 (1974) 537.
[2] B. Pałosz, W. Pałosz, S. Gierlotka, Acta Crystallogr. C 41 (10) (1985) 1402.
[3] F.A.S. Al-Alamy, A.A. Balchin, M. White, J. Mater. Sci. 12 (1977) 2037.
[4] B. Pałosz, E. Salje, J. Appl. Crystallogr. 22 (6) (1989) 622.
[5] R.M. Hazen, L.W. Finger, Am. Mineral. 63 (3-4) (1978) 289.
[6] S. Nakashima, H. Katahama, A. Mitsuishi, Physica B+C 105 (1-3) (1981) 343.
[7] R. Mitchell, Y. Fujiki, Y. Ishizawa, J. Cryst. Growth 57 (2) (1982) 273.
[8] B. Pałosz, W. Steurer, H. Schulz, Acta Crystallogr. B 46 (4) (1990) 449.
[9] S. Arora, D.H. Patel, M.K. Agarwal, J. Cryst. Growth 131 (1993) 268.
[10] Y. Zhu, Y. Chen, L. Liu, J. Cryst. Growth 328 (1) (2011) 70.
[11] F. Tan, S. Qu, X. Zeng, C. Zhang, M. Shi, Z. Wang, L. Jin, Y. Bi, J. Cao, Z. Wang, Y. Hou, F. Teng, Z. Feng, Solid State Commun. 150 (2010) 58.
[12] F. Tan, S. Qu, J. Wu, K. Liu, S. Zhou, Z. Wang, Nanoscale Res. Lett. 6 (1) (2011) 298.
[13] P. Wahnon, J.C. Conesa, P. Palacios, R. Lucena, I. Aguilera, Y. Seminovski, F. Fresno, Phys. Chem. Chem. Phys. 13 (2011) 20401.
[14] P.E. Blöchl, Phys. Rev. B 50 (1994) 17953.
[15] G. Kresse, D. Joubert, Phys. Rev. B 59 (1999) 1758.
[16] J.P. Perdew, K. Burke, M. Ernzerhof, Phys. Rev. Lett. 77 (8) (1996) 3865.
[17] J. Heyd, G.E. Scuseria, M. Ernzerhof, Chem. Phys. 118 (2003) 8207.
[18] J. Heyd, G.E. Scuseria, M. Ernzerhof, J. Chem. Phys. 124 (2006) 219906.
[19] S. Grimme, J. Comput. Chem. 27 (15) (2006) 1787.
[20] J.C. Conesa, J. Phys. Chem. C 114 (2010) 22718.
[21] S. Grimme, R. Huenerbein, S. Ehrlich, ChemPhysChem 12 (2011) 1258.
[22] S. Acharya, O.N. Srivastava, Phys. Status Solidi A 56 (1) (1979) K1.
[23] G. Domingo, R.S. Itoga, C.R. Kannewurf, Phys. Rev. 143 (1966) 536.